Effect of shell thickness on small-molecule solar cells enhanced by dual plasmonic gold-silica nanorods

Xiaoyan Xu, Qingguo Du, Bo Peng, Qihua Xiong, Lei Hong, Hilmi Volkan Demir, Terence K. S. Wong, Aung Ko Ko Kyaw, and Xiao Wei Sun

Articles you may be interested in

Plasmon-enhanced polymer photovoltaic cells based on large aspect ratio gold nanorods and the related working mechanism
Appl. Phys. Lett. **104**, 213903 (2014); 10.1063/1.4880575

Enhancement of short-circuit current density in polymer bulk heterojunction solar cells comprising plasmonic silver nanowires
Appl. Phys. Lett. **104**, 123302 (2014); 10.1063/1.4869760

Enhanced photocurrent in crystalline silicon solar cells by hybrid plasmonic antireflection coatings
Appl. Phys. Lett. **101**, 261102 (2012); 10.1063/1.4773038

Optical scattering and electric field enhancement from core–shell plasmonic nanostructures
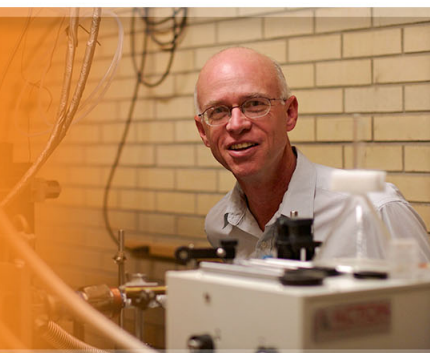J. Appl. Phys. **110**, 103105 (2011); 10.1063/1.3660774

Enhancement of light absorption using high-k dielectric in localized surface plasmon resonance for silicon-based thin film solar cells
J. Appl. Phys. **109**, 093516 (2011); 10.1063/1.3587165

Effect of shell thickness on small-molecule solar cells enhanced by dual plasmonic gold-silica nanorods

Xiaoyan Xu,[1] Qingguo Du,[2] Bo Peng,[3] Qihua Xiong,[3] Lei Hong,[1] Hilmi Volkan Demir,[1] Terence K. S. Wong,[1,a)] Aung Ko Ko Kyaw,[4,b)] and Xiao Wei Sun[1,c)]

[1]*School of Electrical and Electronic Engineering, Nanyang Technological University, Singapore 639798, Singapore*
[2]*Institute of High Performance Computing, 1 Fusionopolis Way, #16-16 Connexis North, Singapore 138632, Republic of Singapore*
[3]*School of Physical and Mathematical Sciences, Nanyang Technological University, Singapore 639798, Singapore*
[4]*Institute of Materials Research and Engineering (IMRE), Agency for Science Technology and Research (A*STAR), Singapore 117602, Republic of Singapore*

Chemically synthesized gold (Au)-silica nanorods with shell thickness of 0 nm–10 nm were incorporated into the bulk heterojunction of a small-molecule organic solar cell. At optimal (1 wt. %) concentration, Au-silica nanorods with 5 nm shell thickness resulted in the highest power conversion efficiency of 8.29% with 27% relative enhancement. Finite-difference time-domain simulation shows that the localized electric field intensity at the silica shell-organic layer interface decreases with the increase of shell thickness for both 520 nm and 680 nm resonance peaks. The enhanced haze factor for transmission/reflection of the organic layer is not strongly dependent on the shell thickness. Bare Au nanorods yielded the lowest efficiency of 5.4%. Light intensity dependence measurement of the short-circuit current density shows that the silica shell reduces bimolecular recombination at the Au surface. As a result, both localized field intensity and light scattering are involved in efficiency enhancement for an optimized shell thickness of 5 nm. © 2014 AIP Publishing LLC. [http://dx.doi.org/10.1063/1.4896516]

Plasmonic organic solar cells (OSCs) have been intensively investigated in recent years in the field of organic photovoltaics.[1–3] Nanoparticles (NPs) of the noble metals, primarily Au and Ag were found to be effective in enhancing the power conversion efficiency (PCE) of both single junction and tandem OSCs through the localized surface plasmon resonance (LSPR) phenomenon.[4–6] Au and Ag NPs have been incorporated by solution processing into the anode buffer (hole transport) layer, active layer, or at the interface of these two layers.[7–9] In addition to the nanosphere, various NP morphologies such as nanorod, nanodisk, and nanoprism had been studied. When chemically synthesized Au or Ag NPs were introduced directly into the photoactive layer, the PCE was observed to either increase slightly or decrease with respect to the reference device despite increased optical absorption and carrier mobility.[10] This effect has been attributed to increased carrier recombination at the surface ligands or surfactants of the chemically synthesized metallic NPs or increased exciton quenching. As a result, core-shell Au and Ag NPs with an insulating silica (SiO_2) shell had been studied for incorporation in the active layer.[11–13] In Ref. 13, a 26% relative enhancement in PCE was observed for a low bandgap polymer:fullerene bulk heterojunction (BHJ) device after incorporation of 1% weight ratio (wt. %) Au-silica nanorods. A similar enhancement was found when Ag-silica NPs were introduced at the interface of the anode buffer layer and active layer of a polymer:fullerene BHJ device.[14]

The thickness of the silica shell is an important design parameter of core-shell noble metal-silica NPs. If the silica shell is too thick, the localized electric field enhancement effect around the NP embedded in the photoactive layer will be greatly diminished. On the other hand, a silica shell that is too thin may result in increased surface recombination. Thus far, there had been no systematic experimental study on the effect of the silica shell thickness on the enhancement mechanism of Au-silica nanorods in plasmonic OSCs. There is also a need to quantitatively compare the surface recombination of bare and core shell Au-silica NPs within a BHJ.

In this paper, we studied the effect of the silica shell thickness of Au-silica nanorods on the performance of solution-processed small-molecule (SM) BHJ OSCs consisting of 7,7′-(4,4-bis(2-ethylhexyl)-4H-silolo[3,2-b:4,5-b′]-dithiophene-2,6-diyl)bis(6-fluoro-4-(5′-hexyl-[2,2′-bithiophen]-5-yl)benzo[c][1,2,5]thiadiazole):[6,6]-phenyl-C_{71}-butyric acid methyl ester (p-DTS(FBTTh$_2$)$_2$:PC$_{70}$BM). The choice of nanorods is motivated by the fact that unlike nanospheres, the use of nanorods allows the tuning of the longitudinal LSPR absorption peak to match the absorption spectrum of the donor:acceptor blend.

The SM solar cell with the structure of indium tin oxide (ITO)/Poly(3,4-ethylenedioxythiophene):poly(styrenesulfonate) (PEDOT:PSS)/p-DTS(FBTTh$_2$)$_2$:PC$_{70}$BM/Ca/Ag were fabricated. The p-DTS(FBTTh$_2$)$_2$:PC$_{70}$BM blend and Au-silica nanorods were mixed in chlorobenzene (CB) with 0.4 v/v% 1,8-octanedithiol (DIO) processing additive to form uniform solution. The final solutions consisted of p-DTS(FBTTh$_2$)$_2$ (21 mg/ml) and PC$_{70}$BM (14 mg/ml) and Au-silica nanorods (1 wt. % of the weight of p-DTS(FBTTh$_2$)$_2$:PC$_{70}$BM blend). For all devices,

a)Electronic mail: ekswong@ntu.edu.sg
b)Electronic mail: kyawakk@a-star.imre.edu.sg
c)Electronic mail: EXWSun@ntu.edu.sg

the solutions were spin-coated at 2000 rpm for 45 s in a glove box. All the BHJ films were thermally annealed at 80 °C for 10 min and their thicknesses were determined by a surface profiler to be 100 ± 2 nm. Finally, 20 nm Ca and 80 nm Ag were thermally deposited sequentially under vacuum condition of 1×10^{-4} Pa. All fabricated devices have an active area of 8 mm^2 and were encapsulated before removal from the glove box. A Keithley 2400 source meter unit under simulated 100 mW/cm^2 (AM1.5G) irradiation from a solar simulator was used to obtain the current density-voltage (*J-V*) characteristics. The light intensity dependence of short-circuit current density (J_{SC}) was studied by tuning the light intensity using neutral density filters. The light intensity passing through the filter was confirmed by a power meter. Optical absorption spectra of the thin film samples were measured using a UV/Vis/near-IR spectrophotometer (Perkin Elmer Lambda 950) fitted with an integrating sphere with a diameter of 150 mm. Four types of Au nanorods with the silica shell thicknesses of 0 nm, 5 nm, 7 nm, and 10 nm, respectively, were synthesized using the seed-mediated method for the Au core followed by solution synthesis of the silica shell.[15] The synthesis procedure of Au-silica nanorods is described in detail in the supplementary material.[16] The thickness of the silica shell was increased by increasing the amount of tetraethoxysilane (TEOS) used during synthesis.[17] A JEOL 1400 transmission electron microscope (TEM) with an accelerating voltage of 100 kV was used to obtain bright field images of the NPs.

The TEM images (Figs. 1(a)–1(d)) display that the average length and diameter of the Au nanorod core are approximately 87 nm and 34 nm, respectively. The normalized UV/Vis absorption spectrum (Fig. 1(e)) reveals that Au-silica nanorods with 5 nm of silica shell in CB have a broad absorption spectrum with dual LSPR peaks at 520 nm and 680 nm. The absorption spectrum shifts only 2–3 nm when the shell thickness changes from 5 nm to 10 nm because of a change in the dielectric environment. The major LSPR peak of nanorods at 680 nm is also well-matched with the absorption peak of p-DTS(FBTTh$_2$)$_2$ donor.

Fig. 2(a) represents the *J-V* characteristics of the p-DTS(FBTTh$_2$)$_2$:PC$_{70}$BM devices with and without 1 wt. % of Au nanorods with various silica shell thicknesses under AM1.5G irradiation at 100 mW/cm^2. The concentrations of Au-silica nanorods are optimized at 1 wt. %. The average photovoltaic parameters calculated from ten devices for each type are listed in Table I. The reference device without NPs has an average PCE of $6.5\% \pm 0.14\%$ with the open-circuit voltage (V_{OC}) of 0.77 ± 0.01 V, short-circuit current density J_{SC} of 12.01 ± 0.27 mA/cm^2, and fill factor (*FF*) of $70.2\% \pm 0.32\%$. After incorporation of 1 wt. % bare Au nanorods, the average V_{OC}, J_{SC}, *FF*, and PCE are decreased to 0.72 ± 0.01 V, 11.73 ± 0.13 mA/cm^2, $63.5\% \pm 0.49\%$, and $5.4\% \pm 0.05\%$, respectively. The reduction in PCE is similar to that reported in Ref. 10. Both the reduced *FF* and V_{OC} suggest that the Au nanorods may have acted as charge recombination centers. Upon incorporation of Au-silica nanorods with 5 nm, 7 nm, and 10 nm silica shell, the V_{OC} and *FF* remain the same while the J_{SC} increases to 15.14 ± 0.35 mA/cm^2, 14.53 ± 0.26 mA/cm^2, and 14.12 ± 0.23 mA/cm^2, respectively. The unchanged V_{OC} and *FF* suggest that incorporation of silica coating nanorods
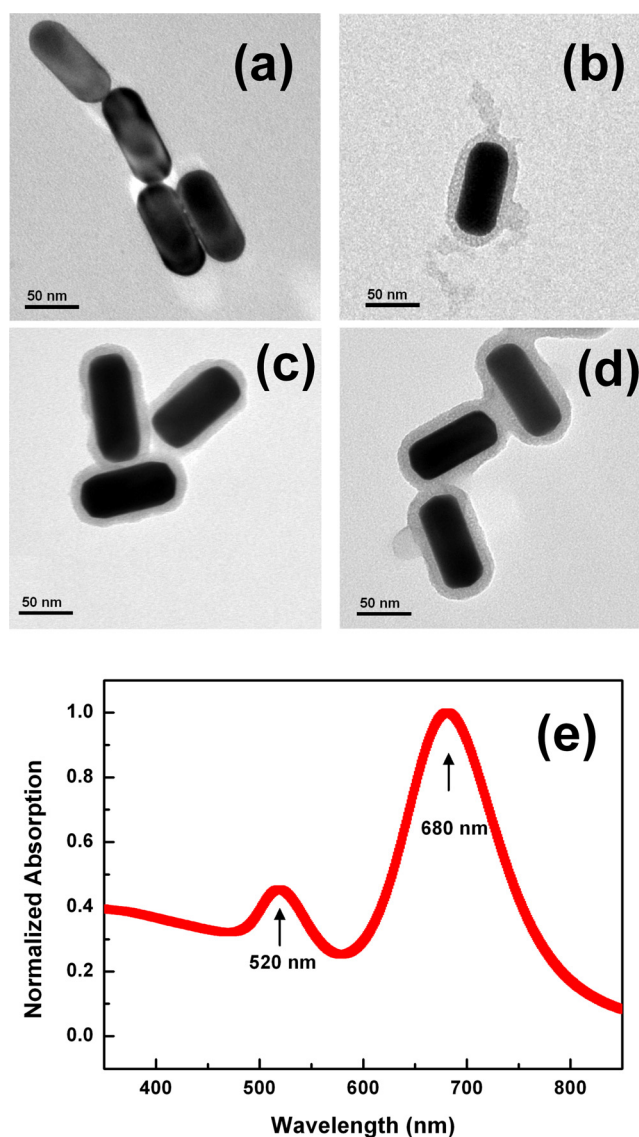

FIG. 1. TEM images of Au nanorods with silica shell thickness of (a) 0 nm, (b) 5 nm, (c) 7 nm, and (d) 10 nm. The scale bars represent 50 nm. (e) Normalized UV/Vis absorption spectrum of Au-silica nanorods with 5 nm silica shell in CB solvent.

does not induce charge recombination. In addition, the improved J_{SC} indicates that light absorption is enhanced by incorporation of Au-silica nanorods, which is confirmed by absorption spectra in Fig. 2(b). Although there are similar enhancement in absorption for all four types of Au nanorods embedded in the p-DTS(FBTTh$_2$)$_2$:PC$_{70}$BM film, the value of J_{SC} decreases somewhat with the increase of the silica shell thickness. These results show the importance of having a silica shell around the Au nanorods and the need to carefully tailor the silica shell thickness during nanorod synthesis.

In order to study the effect of silica shell on the enhanced photocurrent in the p-DTS(FBTTh$_2$)$_2$:PC$_{70}$BM devices, the enhancement mechanisms including the LSPR effect and light scattering were investigated. Localized electric field intensity distributions within the active layer embedded with Au-silica nanorods are simulated by finite-difference time-domain (FDTD) method.[18] The wave is incident from the top and electric field is polarized parallel to the
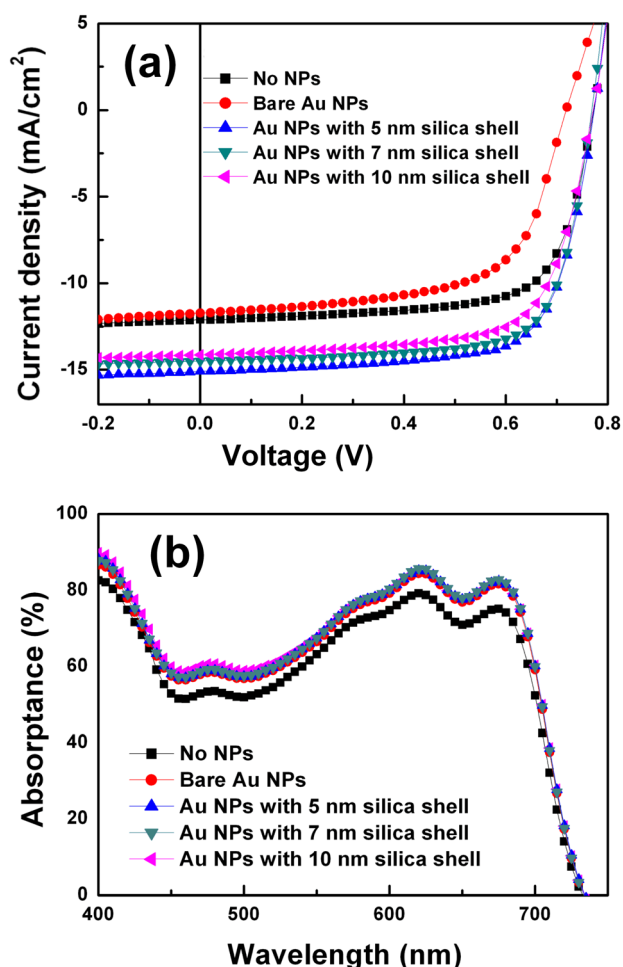
FIG. 2. (a) *J-V* characteristics of p-DTS(FBTTh$_2$)$_2$:PC$_{70}$BM BHJ solar cells incorporated with and without Au nanorods with various silica shell thicknesses and (b) UV/Vis absorption spectra of p-DTS(FBTTh$_2$)$_2$:PC$_{70}$BM BHJ films incorporated with and without Au nanorods with various silica shell thicknesses.

longitudinal axis of the nanorod. The electric field intensity distributions in the active layer embedded with Au-silica nanorod at 520 nm and 680 nm are shown in Fig. 3 for different silica shell thicknesses from 5 nm to 10 nm. From the simulation, for the same thickness, strong electric field localization is observed which is due to LSPR excited by Au-silica nanorod. The electric field intensities are also enhanced around the Au-silica nanorod at both 520 nm and 680 nm. The highly localized electric field corresponds to the broadband light absorption enhancement in the active layer.

For the 5 nm shell thickness illustrated in Fig. 3(a), there is significant enhancement of electric field intensity at the interface of the silica shell and the nearby organic medium

(white dotted line). For the 7 nm shell thickness, the enhancement pattern in Fig. 3(b) is basically similar to that of Fig. 3(a) for both 520 nm and 680 nm. However, at the surface of the silica shell, the electric field intensity enhancement is slightly reduced, which is consistent with the reduced J_{SC} in Fig. 2(a). When the shell thickness is increased to 10 nm (Fig. 3(c)), the electric field intensity distribution at the surface of the Au core is still similar to that of Figs. 3(a) and 3(b) but the electric field intensity enhancement at the surface of the silica shell is greatly reduced. Therefore, the electric field intensity at the surface of the 5 nm silica shell is higher and contributes to more light absorption by organic medium.

Haze factor measurement was performed to examine the dependence of scattering effects of Au nanorods with various shell thicknesses in the SM solar cells. Haze factor for transmission (H_T) and reflection (H_R) are defined as the ratio between the diffuse transmission/reflection and the total transmission/reflection.[19] The H_T and H_R for p-DTS(FBTTh$_2$)$_2$:PC$_{70}$BM film with and without Au-silica nanorods are shown in supplementary material (Fig. S1).[16] Upon incorporating the Au-silica nanorods, there are similar enhancements in H_T and H_R for Au nanorods with 0 nm, 5 nm, 7 nm, and 10 nm. It can be seen that the silica shell thickness has little effect on both H_T and H_R. Such enhancements show that the light scattering is increased in the active layer when incorporating the Au-silica or Au nanorods. Taken together, it can be concluded that both LSPR effect and the scattering effects excited by Au-silica nanorods with 5 nm silica shell attribute to the light absorption enhancement. This also suggests that for shell thickness of 10 nm or more, the electric field intensity enhancement in the vicinity of the nanorod is negligible and enhancement is dominated by scattering.

As mentioned above, the J_{SC}, V_{OC}, and FF decreased after incorporation of bare Au nanorods, while the J_{SC} increased and V_{OC} and FF remained unchanged for Au-silica nanorods. In order to further understand the effect of silica shell on the device performance, we studied the recombination mechanisms influenced by Au nanorods with and without silica shell by measuring the J_{SC} at various light intensities. Generally, J_{SC} of OSC device follows a power law dependence on the illumination light intensity, which can be written as[20,21]

$$J_{SC} \propto P^S, \tag{1}$$

where P is light intensity and S is the exponential factor. Ideally, the value of S should be 1 for a solar cell without any bimolecular recombination. The value of S, however, is usually less than 1 for OSC due to bimolecular recombination

TABLE I. Photovoltaic device parameters of SM BHJ devices based on p-DTS(FBTTh$_2$)$_2$:PC$_{70}$BM with and without 1 wt. % of Au nanorods with various silica shell thicknesses under 100 mW/cm^2 AM1.5G simulated solar irradiation.

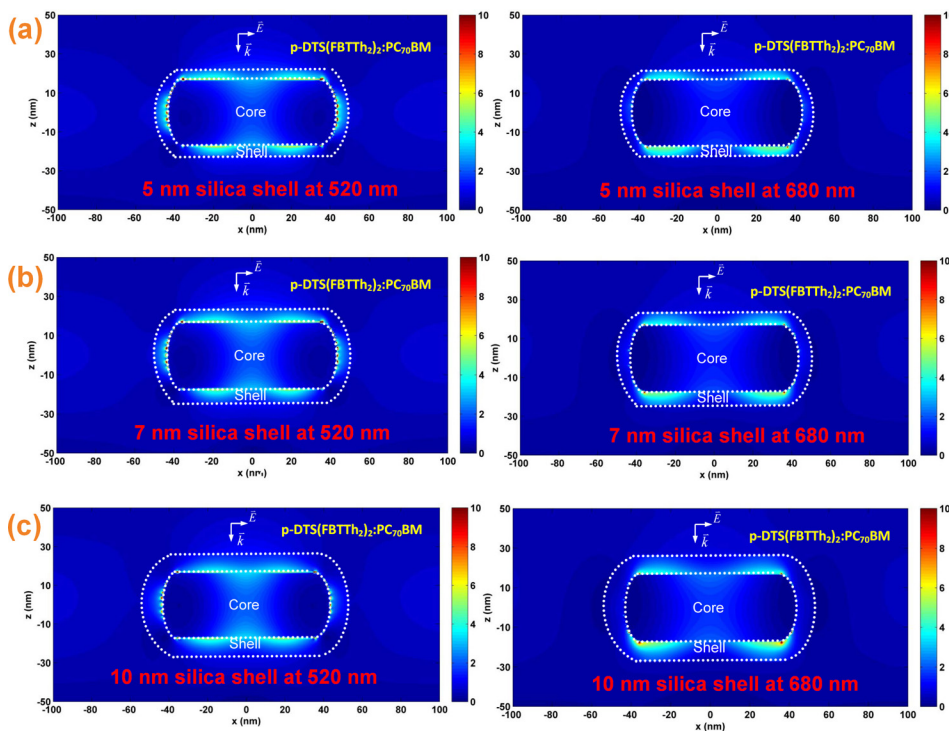| Au nanorods shell thickness (nm)	V_{OC}(V)	J_{SC} (mA/cm^2)	FF (%)	PCE (%)
No NPs	0.77 ± 0.01	12.01 ± 0.27	70.2 ± 0.32	6.5 ± 0.14
0	0.72 ± 0.01	11.73 ± 0.13	63.5 ± 0.49	5.4 ± 0.05
5	0.77 ± 0.01	15.14 ± 0.35	70.4 ± 0.61	8.2 ± 0.12
7	0.77 ± 0.01	14.53 ± 0.26	70.3 ± 0.43	7.8 ± 0.12
10	0.77 ± 0.01	14.12 ± 0.23	70.2 ± 0.41	7.6 ± 0.10

FIG. 3. Electric field intensity distributions of Au-silica nanorods at 520 nm and 680 nm for (a) 5 nm silica shell, (b) 7 nm silica shell, and (c) 10 nm silica shell.

which is unavoidable in low mobility materials such as organic solids. From Fig. 4, the value of $S = 0.913$ and $S = 0.944$ for bare Au nanorods and Au nanorods with 5 nm silica shell, respectively, were determined by fitting the data with Eq. (1). A higher value of S indicates that bimolecular recombination which is likely to occur at the surface of metallic nanorod is reduced for the device with silica coated Au nanorods. This reduced bimolecular recombination is consistent with the increase in J_{SC} and FF in the device with silica coated Au nanorod.

In conclusion, we improved the PCE of solution-processed SM solar cells by incorporation of Au-silica nanorods into p-DTS(FBTTh$_2$)$_2$:PC$_{70}$BM active layer. At the optimized concentration of 1 wt. % Au-silica nanorods with 5 nm silica shell, J_{SC} and PCE increased by ∼25% and ∼27%, respectively. FDTD simulation reveals that shell thickness should be thin to enable sufficient localized electric field intensity outside the silica shell. However, the silica shell must be present due to the otherwise increased bimolecular recombination at the Au surface as demonstrated by the light intensity dependence of J_{SC}. PCE enhancements in SM BHJ solar cells incorporated with nanorods with 5 nm silica shell is due to both LSPR and scattering effects.
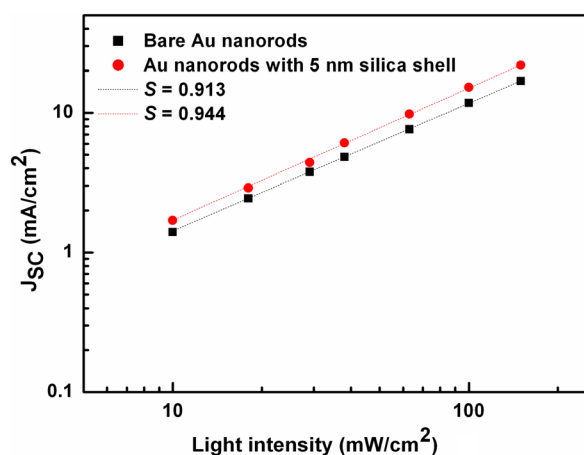
FIG. 4. The value of J_{SC} as a function of light intensity for bare Au nanorods and Au nanorods with 5 nm silica shell. Short dash lines are fitted by Eq. (1).

[1]K. R. Catchpole and A. Polman, Opt. Express **16**, 21793–21800 (2008).
[2]H. A. Atwater and A. Polman, Nat. Mater. **9**, 205–213 (2010).
[3]V. E. Ferry, J. N. Munday, and H. A. Atwater, Adv. Mater. **22**, 4794–4808 (2010).
[4]F.-C. Chen, J.-L. Wu, C.-L. Lee, Y. Hong, C.-H. Kuo, and M. H. Huang, Appl. Phys. Lett. **95**, 013305 (2009).
[5]J.-L. Wu, F.-C. Chen, Y.-S. Hsiao, F.-C. Chien, P. Chen, C.-H. Kuo, M. H. Huang, and C.-S. Hsu, ACS Nano **5**, 959–967 (2011).
[6]J. Yang, J. You, C.-C. Chen, W.-C. Hsu, H.-R. Tan, X. W. Zhang, Z. Hong, and Y. Yang, ACS Nano **5**, 6210–6217 (2011).
[7]L. Lu, Z. Luo, T. Xu, and L. Yu, Nano Lett. **13**, 59–64 (2013).
[8]C. C. D. Wang, W. C. H. Choy, C. Duan, D. D. S. Fung, W. E. I. Sha, F. X. Xie, F. Huang, and Y. Cao, J. Mater. Chem. **22**, 1206–1211 (2012).
[9]F. X. Xie, W. C. H. Choy, C. C. D. Wang, W. E. I. Sha, and D. D. S. Fung, Appl. Phys. Lett. **99**, 153304 (2011).
[10]M. Xue, L. Li, B. J. Tremolet de Villers, H. Shen, J. Zhu, Z. Yu, A. Z. Stieg, Q. Pei, B. J. Schwartz, and K. L. Wang, Appl. Phys. Lett. **98**, 253302 (2011).
[11]M. D. Brown, T. Suteewong, R. S. S. Kumar, V. D'Innocenzo, A. Petrozza, M. M. Lee, U. Wiesner, and H. J. Snaith, Nano Lett. **11**, 438–445 (2011).

[12] D. H. Wang, D. Y. Kim, K. W. Choi, J. H. Seo, S. H. Im, J. H. Park, O. O. Park, and A. J. Heeger, Angew. Chem. Int. Ed. **50**, 5519–5523 (2011).

[13] X. Xu, A. K. K. Kyaw, B. Peng, D. Zhao, T. K. S. Wong, Q. Xiong, X. W. Sun, and A. J. Heeger, Org. Electron. **14**, 2360–2368 (2013).

[14] H. Choi, J.-P. Lee, S.-J. Ko, J.-W. Jung, H. Park, S. Yoo, O. Park, J.-R. Jeong, S. Park, and J. Y. Kim, Nano Lett. **13**, 2204–2208 (2013).

[15] T. Ming, L. Zhao, Z. Yang, H. Chen, L. Sun, J. Wang, and C. Yan, Nano Lett. **9**, 3896–3903 (2009).

[16] See supplementary material at http://dx.doi.org/10.1063/1.4896516 for (1) synthesis of Au-silica nanorods in detail and (2) Fig. S1 showing (a) H_T spectra and (b) H_R spectra for p-DTS(FBTTh$_2$)$_2$:PC$_{70}$BM films with and without 1 wt. % Au-silica nanorods with silica shell thickness of 0 nm, 5 nm, 7 nm, and 10 nm.

[17] B. Peng, Q. Zhang, X. Liu, Y. Ji, H. V. Demir, C. H. A. Huan, T. C. Sum, and Q. Xiong, ACS Nano **6**, 6250–6259 (2012).

[18] N. Lagos, M. M. Sigalas, and E. Lidorikis, Appl. Phys. Lett. **99**, 063304 (2011).

[19] Y.-S. Hsiao, C.-P. Chen, C.-H. Chao, and W.-T. Whang, Org. Electron. **10**, 551–561 (2009).

[20] V. D. Mihailetchi, H. X. Xie, B. de Boer, L. J. A. Koster, and P. W. M. Blom, Adv. Funct. Mater. **16**, 699–708 (2006).

[21] P. Schilinsky, C. Waldauf, and C. J. Brabec, Appl. Phys. Lett. **81**, 3885–3887 (2002).